Low Complex OFDM Synchronization in Power Line Communication for Flight Control System in Aircraft

Jean-Yves Baudais[1], Fabienne Nouvel[2], Thomas Larhzaoui[3]

Institute of Electronics and Telecommunications of Rennes (IETR), UMR CNRS 6164, Rennes, France

***Abstract*—** *The flight control system (FCS) over power line communication (PLC) is subject to strong real time constraints and harsh aircraft operating conditions. Then, low complex and accurate synchronization procedure have to be adapted. In this paper, we propose a synchronization procedure performed in two phases and we focus on the operating phase with a synchronization using the received data to estimate the sampling frequency offset. This estimation is performed by using two estimators based on the maximum likelihood principle. The first estimator performs the estimation on one orthogonal frequency division multiplexing (OFDM) transmission symbol. The second estimator performs the estimation on 20 successive OFDM symbols and uses the estimation of the previous estimator. The performances of the estimator are compared to the Cramér-Rao lower bound (CRLB). The proposed synchronization procedure reached the CRLB and satisfies the FCS constraints over PLC.*

***Keywords*— PLC, OFDM, avionics, aircraft, sampling frequency synchronization, Cramér-Rao lower bound, maximum likelihood, safety critical systems, HVDC network.**

I. INTRODUCTION

A lot of previous works deal with the question of synchronization in orthogonal frequency-division multiplexing (OFDM) [1–3] and digital multi-tone (DMT) [4], applied to power line communication (PLC) systems [5,6]. Many solutions are based on pilot sub-carriers which allows to have the parameter estimation at each OFDM symbol [7–9]. In this case, some sub-carriers are kept for the synchronization. Another possibility is to use OFDM pilot symbols. These OFDM pilot symbols are sent regularly to estimate the sampling time and frequency offset. For example, the Schmidl-Cox algorithm [10] and its improvement [11–13] allows such kind of estimation and sampling frequency offset correction with one or two OFDM symbols. The high synchronization accuracy, compatible with OFDM transmission, can then be reached using common oscillator in electronic systems [14].

The power line communication (PLC) has been proposed for the flight control system (FCS) in aircrafts to reduce the wiring complexity [15]. The OFDM transmission has been proposed [16, 17] to ensure the security requirement, which is undamental in FCS. The FCS transmission must satisfy unfavorable conditions and should be deterministic, non-sporadic, continuous and with low latency adapted to the FCS loop. Conventional communication techniques cannot be used in this context. For example, the reliability enhancement with retransmission mechanisms is not possible. In the case of shared channel between multiple transmitters or receivers, the multiple access strategy should be deterministic. Concerning the synchronization procedure, the pilot symbols are not compatible with the continuity requirement and increase adversely the latency. Furthermore, the pilot sub-carriers yield to a bit-rate reduction and are not suitable in secure high bit-rate. The constraints of FCS have been taken into account to design an OFDMPLC system [17], but the synchronization should also be adapted to this specific FCS. Moreover, and under operating conditions, temperature variations and vibrations induce a drift between the local transmitter and receiver oscillators which can cause a sampling frequency offset.

Considering all theses constraints, we propose to synchronize the receiver in two different phases: the initialization phase and the operating phase. During the initialization phase, no transmission is needed for FCS. The PLC system has enough time to ensure accuracy of synchronization in the range of one ppm [14]. Conventional OFDM synchronization algorithms can then be used in the first phase. In this paper, we propose to design the synchronization system of the operating phase, using the transmitted data. This allows us to propose a synchronization procedure with a better spectral efficiency than a system using pilot sub-carriers or pilot symbols. A simple and low complex asymptotic unbiased estimation based on the maximum likelihood (ML) is derived and proposed. To increase the robustness of the synchronization strategy, a super-frame structure is proposed, which allows a re-estimation of the channel and a resynchronization with an accuracy of one ppm at the beginning of each super-frame. The interest to consider a super-frame is to have a long stable period and to propose a simple synchronization system during the operating phase. Note that, no carrier frequency offset is considered and the PLC signal is a base band signal which means that no frequency transposition has to be done and corrected.

The paper is organized as follows. In Section II, the channel model and the communication system used are presented. Section III describes the synchronization errors of the used system. The synchronization strategy is described in Section IV and Section V focuses on the characterization of the operating phase synchronization. Finally, conclusion is given in Section VI.

II. COMMUNICATION MODELS

2.1 Propagation Channel

The considered PLC channel of FCS is the power line between the electronic control unit and the motor control unit using the high voltage direct current (HVDC). The point-to-multipoint network and return channel for monitoring can be envisaged. In that case, deterministic time division multiple access (TDMA) and time division duplex (TDD) ensure multiple access and duplex compatible with FCS. However, the features of the TDMA and TDD system are unknown because the HVDC network is still under design. In the following, we do not consider time sharing and the communication is assumed to be unidirectional. The results and the synchronization strategy presented in this paper remain valid in the case of deterministic point-to-multipoint networks.

Fig. 1 shows the network architecture. In this article we focus on a point-to-point architecture with inductive couplers to connect to the HVDC network. To improve the robustness of the system against the noises, it has been chosen to connect the couplers on only one polarity [16]. In our case, the couplers are plugged on the plus polarity. This polarity is short circuited at both end and twisted. The harness is then composed of one twisted pair end one wire and the channel is composed of two inductive couplers and one 32 m long twisted pair. Inductive couplers are composed of one primary coil, one secondary coil and one magnetic torus. Transmission and function transfer measurement are done between V_1 and V_2.

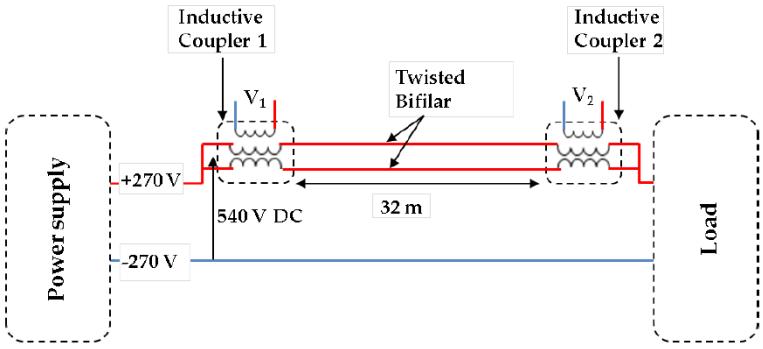

FIGURE 1: NETWORK ARCHITECTURE

Fig. 2 represents insertion gain of the propagation channel in the [1;100] MHz frequency bandwidth. The insertion gain first decreases linearly (in dB) with the frequency up to 40 MHz, and varies from -5 to -25 dB. Then, the insertion gain remains nearly constant between 40 and 80MHz and, beyond 80MHz, decreases very rapidly. Thus, given the insertion gain values, only the first third of the frequency bandwidth is used as shown in the previous studies [16,17].

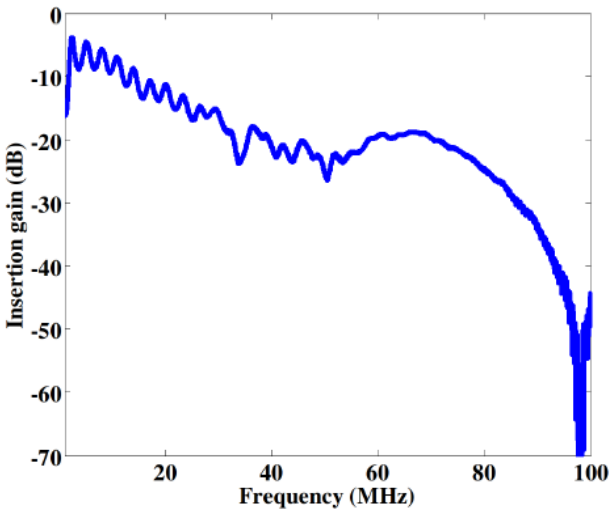

FIGURE 2: INSERTION GAIN OF THE CHANNEL

2.2 Communication System

The parameters of the communication system are presented in Table 1. These parameters come from previous studies whose the purpose was to design the OFDM symbol parameters to comply with the real time, bit rate, bit error rate (BER) and electromagnetic compatibility constraints [17]. To comply with the real time constraint the OFDM symbol duration has been minimized, decreasing the cyclic prefix (CP) duration and increasing the sub-carrier spacing. To find the best compromise between the BER and the bit rate, we have proposed to use the 256 sub-carriers with the best signal to noise ratio (SNR) in the [1;36] MHz bandwidth and to use a quadrature phase-shift keying (QPSK) modulation.

TABLE 1
SYSTEM PARAMETERS

Parameters	Value
CP, ns (nb of sample)	555 (20)
Total frequency bandwidth, MHz	[0;36]
Useful frequency bandwidth, MHz	[1;36]
BER without channel coding	$\leq 10^{-3}$
Total number of sub-carriers	512
Useful number of sub-carriers	256
Constellation	QPSK
Equalization	Zero forcing
E_b/N_0, dB	10
Topology	Point-to-point
Communications	Unidirectional, continuous

III. CHARACTERIZATION OF THE SYNCHRONIZATION ERRORS

In this section, we analyze the errors involved in the synchronization phase. We consider a maximum value of the drift between the local oscillators equal to 100 ppm, which takes into account the harsh operating conditions of the aircraft equipment such as temperature or vibrations for components on the self oscillators. First, assuming an ideal fast Fourier transform (FFT) windowing, the impact of the stretching or contraction of the frequency comb is discussed. Then, the errors due to a wrong FFT windowing are characterized without taking into account the errors due to the frequency comb. The sampling frequency errors appear because the transmitted signal is generated using $(1+\epsilon_f)T_e$ sampling period instead of T_e used at receiver side. The relative error of the sampling frequency is ϵ_f.

3.1 Stretching or Contraction of the Frequency Comb

The m^{th} received OFDM symbol, composed of N sub-carriers, is

$$r_m = F^{-1}(\epsilon_f) H X_m + b_m \tag{1}$$

where

- $F(\epsilon_f)$ is the Fourier matrix F modified by the frequency sampling error ϵ_f , with element $(i , j) \epsilon [0,N-1]^2$ given by

$$\left[F(\epsilon_f)\right]_{i,j} = e^{-2\pi J(1+\epsilon_f)\frac{ij}{N}} \tag{2}$$

- H is the diagonal matrix of the channel with H=diag (Fh^T), where h = [h_1, h_2…… h_n, 0,….,0] is the vectors of the channel coefficients of dimension 1×N with n discrete paths $(h_i)_{i=1}^{n}$.
- Xm is the m^{th} OFDM emitted symbol, expressed in the frequency domain and composed of N QPSK symbols;
- bm is the additive white Gaussian noise.

The signal received after the FFT is:

$$Y_m = FF^{-1}(\epsilon_f)HX_m + Fb_m \tag{3}$$

Fig. 3 represents the BER according to the E_b/N_0 for a sampling frequency error of 0 ppm and 100 ppm. These results are done on one OFDM symbol and the FFT windowing is assumed ideal. This simulation shows no BER difference between 0 ppm and 100 ppm of error. The stretching or the contraction of the frequency comb then have no impact on the BER. However, the error induces a FFT drift which should be characterized and corrected.

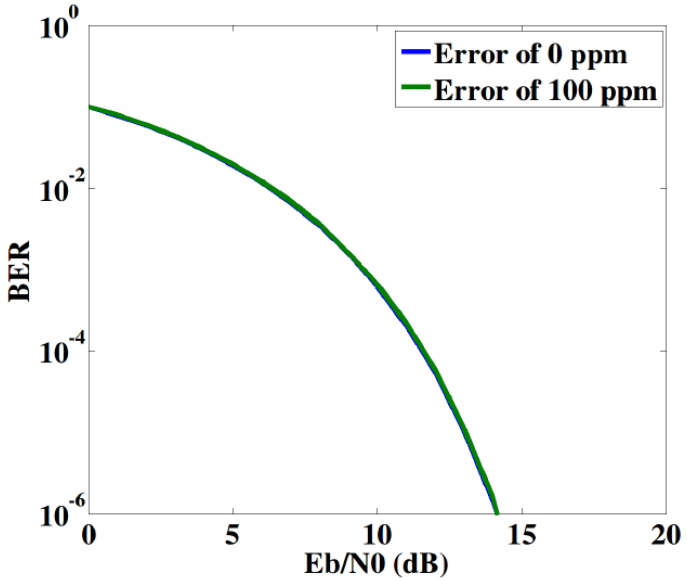

FIGURE 3: IMPACT OF SAMPLING FREQUENCY OFFSET ON THE BER

3.2 Windowing FFT Errors

Fig. 4 shows the four different FFT windowings:

- Case 1 is a late FFT window. This error involves inter-symbol interference (ISI) and inter-carrier interference (ICI);
- Case 2 is the ideal case where the FFT window shift is equal to zero;
- Case 3 is slightly ahead of the FFT window. Assuming that the CP is oversized, the first sample selected by the windowing belongs to the portion of the guard interval that is not affected by the ISI. This area is called the free ISI area. Because of the cyclic nature of the discrete Fourier transform, an offset slightly ahead simply introduces a phase rotation in the frequency domain. This error can be corrected by the equalizer

Case 4 is an important ahead of the FFT window. The first selected samples are then taken in the area which does not absorb the ISI. In addition to a phase rotation, ISI and ICI appear.

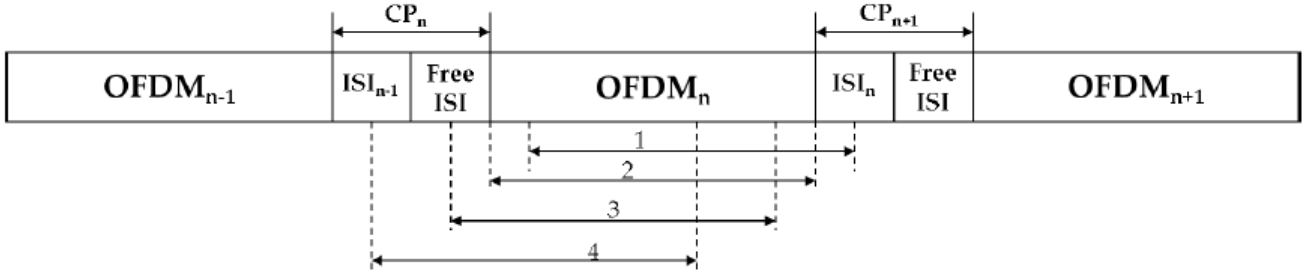

FIGURE 4: DIFFERENT CASES OF FFT WINDOWING

Fig. 5 shows the BER for different cases ahead of the FFT window with correction of the phase rotation. For five samples ahead, there is almost no variation of the BER. For ten samples ahead, there is a slight increase of the BER and for 15

samples ahead, the increase of the BER is quite significant because the selected samples are disturbed by the ISI. These values have to be compared to the CP size given in Table 1. Thus, an ahead of five samples is a good compromise to avoid cases 1 and 4.

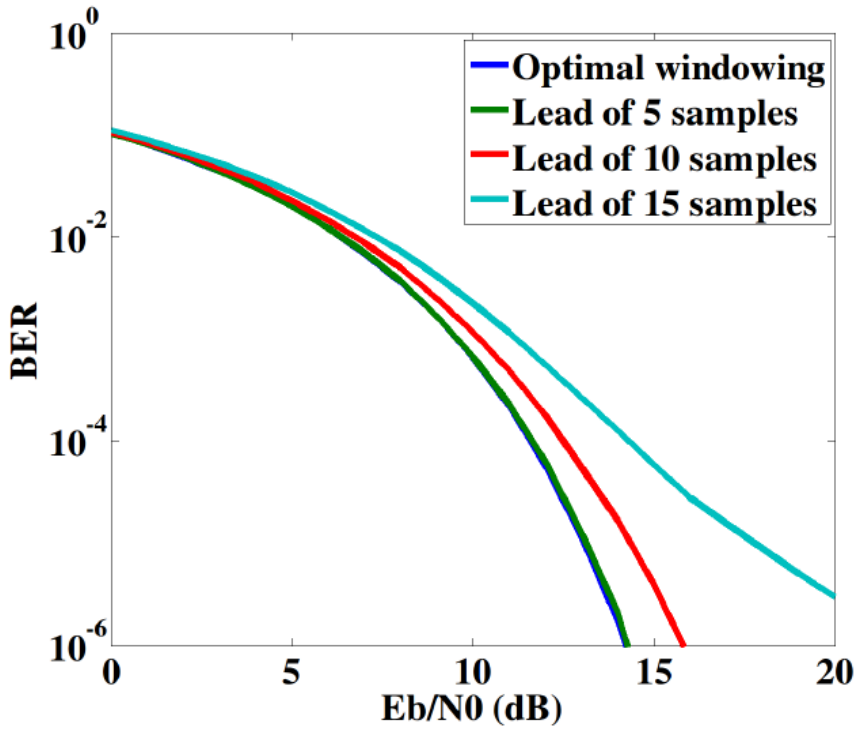

FIGURE 5: BER FOR THE DIFFERENT FFT POSITIONS

If a continuous series of OFDM symbol is considered, the frequency sampling offset induces drift of the FFT windowing. Conversely, if the sampling is too slow, and therefore $\epsilon_f > 0$, this drift induces a delay of the FFT windowing. For an OFDM symbol constituted of $N+N_{CP}$ samples, where N_{CP} is the size of the cyclic prefix in number of samples, the drift ϵ_m is

$$\epsilon_m = \frac{m(N+N_{\mathrm{CP}})\epsilon_f}{N} \tag{4}$$

Note that $m = 0$ corresponds to the OFDM symbol with the FFT window in the proper position equivalent to case 2. Considering the parameters shown in Table 1 and an error ϵ_f of 1 ppm, ϵ_m is equal to 1.04 ppm for $m = 1$. If it is assumed that the FFT windowing is in case 3, the signal in reception after FFT is:

$$Y_m = FF^{-1}(\epsilon_f)\Theta(\epsilon_m)HX_m + Fb_m \tag{5}$$

with $\Theta(\epsilon_m) = \mathrm{diag}(1, e^{2\pi J\epsilon_m}, \cdots, e^{2\pi J(N-1)\epsilon_m})$.

According to Fig. 3, $F(\epsilon_m)$ can be approximated by F and only ϵ_m has to be corrected. The integer part of ϵ_m corresponds to an FFT shift of a number of samples while the decimal part is the phase rotation of each sub-carrier proportional to its index.

To characterize the synchronization error due to a wrong FFT windowing, a transmission of 20 successive OFDM symbols is simulated, as shown in the Fig. 6, and assuming that the beginning of the first symbol of this transmission is synchronized.

FIGURE 6: CONTINUOUS OFDM TRANSMISSION

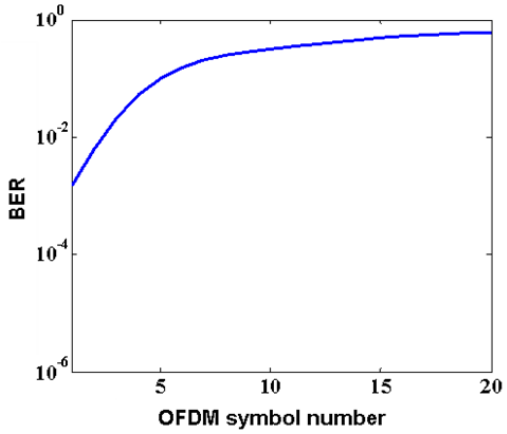

FIGURE 7: BER ACCORDING TO THE OFDM SYMBOL NUMBER

Fig. 7 shows the BER degradation, according to the OFDM symbol number for a sampling frequency offset of 100 ppm and without correction of the phase rotation and the time delay during the 20 successive OFDM symbols. The BER increases with the OFDM symbol number and, after 8 OFDM symbols, the BER is higher than 10¡1. It is then necessary to correct the sampling frequency offset to ensure an acceptable BER.

3.3 Accuracy Requirements

Fig. 8 represents the BER according to the FFT drift ϵ_m for m=1, considering only one OFDM symbol. The BER is quite constant until 50 ppm. Thus, to ensure the stability of the PLC system, the estimation of the sampling frequency offset should be done with an accuracy of 1 ppm after an initialization phase. This allows us to let the system drift during several tens of OFDM symbols, and then to performa correction of the FFT windowing when the error is equal to one sample. Note that the FFT drift is cumulative: an offset of 1 ppm corresponds to an offset of 300 ppm on the 300th OFDM symbol.

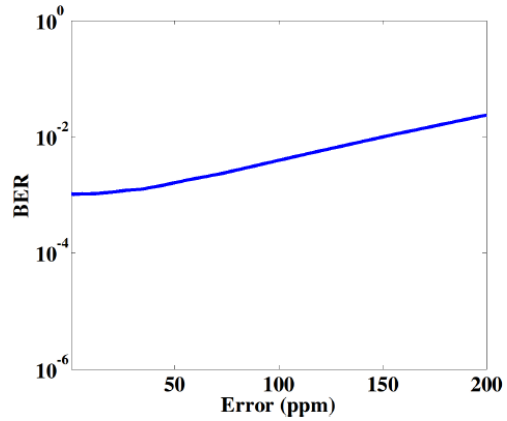

FIGURE 8: BER ACCORDING TO THE OSCILLATORS DRIFT IN PPM

IV. SYNCHRONIZATION STRATEGY

In this section, a general procedure of the estimation of the FFT drift due to the sampling frequency synchronization is proposed.

4.1 Initialization Phase

The purpose of the initialization phase is to make an accurate estimation of the propagation channel and of the sampling frequency offset ϵ_f . It can be assumed that, at the switching of the aircraft, the PLC system have enough time to send several OFDM pilot symbols to estimate the channel coefficients and to synchronize the communication system. It is assumed that the accuracy of the local estimators is in the range of one ppm at the end of this initialization phase [14].

4.2 Operating Phase

In Section III, it has been shown that only the FFT window drift has an impact on the BER. Thus, we propose to only correct the FFT window drift during the operating phase, after the initialization phase. However, during the different flight phases, the temperature between the transmitter and the receiver could vary a lot. Without physical models about these variations, it

is safer to re-estimate the sampling frequency offset, and the channel coefficients, with OFDM pilot symbols. For example, the temperature at the ground level could be around 50 °C. After, during the cruising flight, the temperature is around -60 °C which imply a temperature range of 110 °C. To solve this problem, we propose to use a super-frame in which the temperature is assumed stable. This super-frame structure is only used to provide more security without increased the latency of the FCS loop.

4.3 Super-Frame Structure

To deal with the local oscillator drift due to temperature variation, we propose the synchronization and the channel estimation with OFDM pilot symbols at the beginning of each super-frame whose duration is set to 10 s. An OFDM symbol duration of 15 µs has been proposed in Section III, that implies a super-frame composed of 666667 OFDM symbols. It is assumed that the thermal transfers are slow, i.e. less than one Celsius degree for 10 s, and the channel of propagation is stable during this period. Thus, at the beginning of each super-frame, the channel estimation could be assumed perfect and the drift between the local oscillators in the range of 1 ppm. These values are assumed almost constant for the duration of a super-frame. Taking into account, for example, Schmidl & Cox algorithm and its improvements, one or two OFDM symbols are enough to estimate the sampling frequency offset at the beginning of each super-frame. Thus, the duration of the synchronization phase at the beginning of each super-frame will then be negligible given the duration of a super-frame.

However, inside a super-frame, the FFT windowing will drift. To correct this drift, a low complex algorithm with low latency is developed to estimate the sampling frequency offset on the phase of the received data. The objective is to not decrease the bit rate unlike in the OFDM pilot symbols or pilot sub-carriers.

V. OPERATING PHASE SYNCHRONIZATION

5.1 Synchronization on the Received Data

Synchronization using the received symbols aims to estimate ^{2}m that represents the phase shift between the data after equalization and the received data demapped and remapped. The demapped and remapped data are X'_m and X''_m respectively in Fig. 9. According to the synchronization procedure represented in this Fig. 9, the synchronization for the operating phase is performed in two steps:

1. A correction is performed during the equalization using the decimal part of ϵ_m, which is ϵ_m-[ϵ_m];
2. The FFT window correction is equal to the integer part [ϵ_m] of ϵ_m.

Because the beginning of the FFT window is in the free ISI zone, a shift of some OFDM samples is equivalent in the frequency domain to a phase rotation which is known and equal to five samples, as proposed in Section IV. However, the FFT window has to be corrected to ensure free ISI.

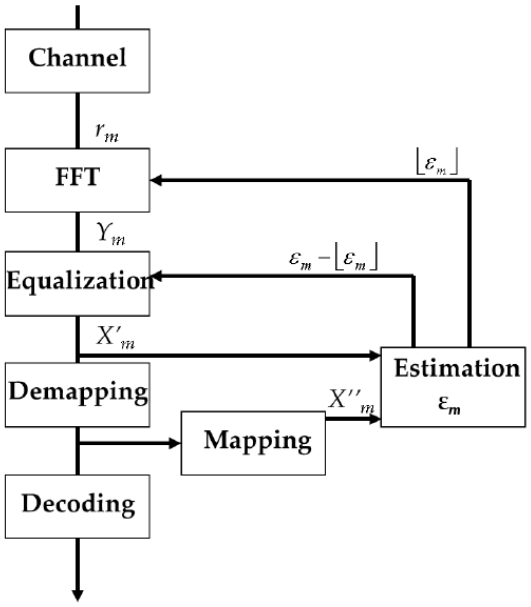

FIGURE 9: SYNCHRONIZATION FOR THE OPERATING PHASE

A biased estimator based on the maximum likelihood is used to estimate ϵ_m:

$$\hat{\epsilon}_m = \frac{\sum_{k\in I} k\Delta\phi}{2\pi \sum_{k\in I} k^2} \tag{6}$$

where ϵ_m is the estimated value of ϵ_m of one OFDM symbol, $\Delta\phi$ is the phase difference between X'_m and X''_m and I is the set of the 256 best active sub-carriers of one OFDM symbol. To evaluate the performance of this estimator, the bias and the variance are calculated.

5.2 Bias Of The Estimator

The estimation of the phase of the received data need to assume that the BER is about 10^{-3} which means that, on average, less than one bit per OFDM symbol is false. This implies that the estimator is asymptotically unbiased according to the E_b/N_0. Fig. 10 represents the bias of the estimator according to E_b/N_0. This bias tends towards zero when E_b/N_0 tends towards infinity and the bias is equal to 1 % at 13 dB and 5 % at 10 dB.

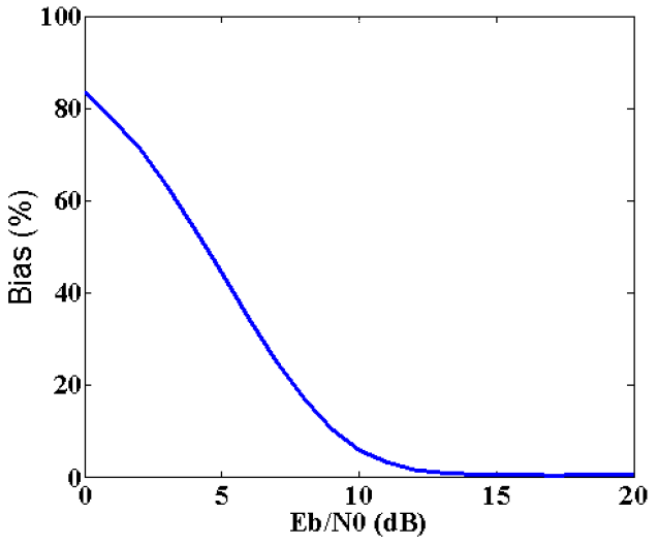

FIGURE 10: BIAS OF THE ESTIMATOR ACCORDING TO E_b/N_0

The bias calculation is done on a very large number of samples but, in the operating conditions, the estimation is done on only one OFDM symbol. To evaluate the dispersion of the estimated values and thus the estimator performance, it is necessary to calculate the estimator variance.

5.3 Variance of the Estimator

The estimator variance depends on its design, thus it is interesting to calculate the estimator variance without taking into account the design to achieve the maximal performance of this kind of estimation. The minimal variance of a unbiased estimator is given by the Cramér-Rao lower bound (CRLB) [18]. The CRLB is given by:

$$\mathrm{var}(\hat{\epsilon}_m) = \frac{\sigma^2}{\sum_{i=0}^{N-1} \left(\frac{\partial}{\partial \epsilon_m} \Re(s(i,\epsilon_m)) + \frac{\partial}{\partial \epsilon_m} \Im(s(i,\epsilon_m)) \right)^2} \tag{7}$$

With σ^2 the variance of the additive white Gaussian noise and $s(i, \epsilon_m)$ is the i^{th} coefficient of the vector $\Theta(\epsilon_m)HX$. This lower bound is an asymptotic lower bound of the proposed estimator because it considers unbiased data, obtained for infinite SNR in practice.

After development, it leads to:

$$\mathrm{var}(\hat{\epsilon}_m) = \frac{\sigma^2}{8\pi^2 \sum_{i\in I} |iH(i)X(i)|^2} \tag{8}$$

where $H(i)$ is the i^{th} diagonal element of the matrix H.

Fig. 11 represents the unbiased CRLB and the variance of the estimator for $m = 1$, and on one OFDM symbol. Because the estimator is biased at low E_b/N_0, the variance of the estimator is lower than the unbiased CRLB below an E_b/N_0 of 8 dB. The variance of the maximum likelihood estimator based on the phase of the received data is very close to the unbiased CRLB which is equivalent to the maximum likelihood when the received data are assumed to be known. Thus, the proposed estimator shows a very good trade-off between the complexity and the performance. The variance is about 10¡9 with an E_b/N_0 of 10 dB. To have accuracy in the range of one ppm, which means estimate an error in the range of 10¡6, the estimation with only one OFDM symbol is not sufficient.

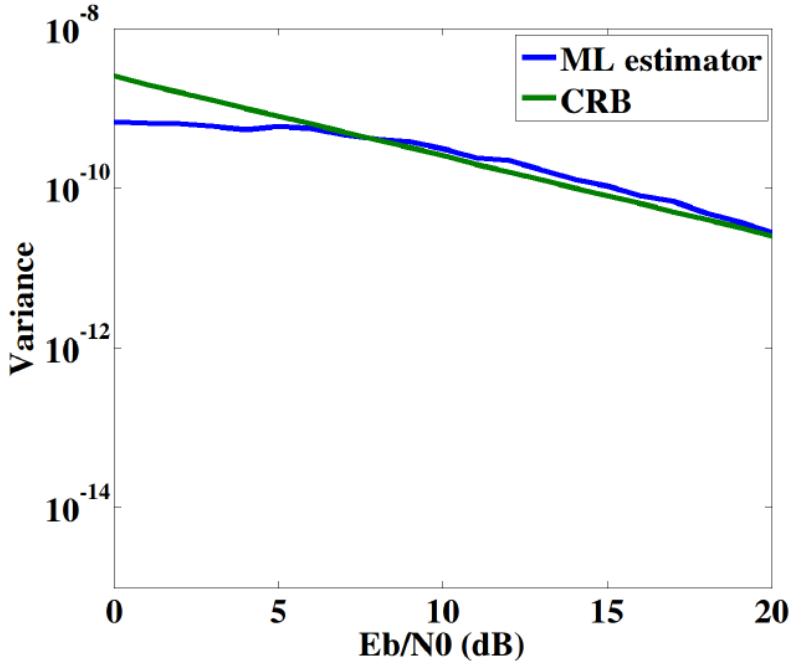

FIGURE 11: CRAMER-RAO BOUND AND VARIANCE OF THE ESTIMATOR ACCORDING TO E_b/N_0

The bias and the variance are evaluated using 256 active sub-carriers with the best SNR. An higher number of active sub-carriers decreases the variance [14], but it also increases the bias. The choice of the number of sub-carriers with the best SNR results of a compromise between variance and bias. To improve the performance of the error estimation, we propose to estimate the frequency error with not only one OFDM symbol but with several OFDM symbols.

5.4 Improvement of the Estimator

The FFT window offset is cumulative from one symbol to another. Considering an estimation error of ϵ_f in the range of 1 ppm, it is possible to not correct the FFT windowing drift during several OFDM symbols without impacting the BER, as shown in Fig. 5, and to use these symbols to have multiple estimations of the same error. This technique allows decreasing the variance of the estimator. It is assumed that inside a super-frame, the variation of ^2f is negligible, i.e. lower than 1 ppm. As for the previous estimator, the ML is used to estimate the FFT windowing shift:

$$\hat{\epsilon}'_M = \frac{\sum_{m=1}^{M} \hat{\epsilon}_m}{\sum_{m=1}^{M} m^2} \tag{9}$$

where ϵ'_M is the estimated value of ϵ_m / m on M OFDM symbols and ϵ_m is given by (6).

Fig. 12 represents the variance of the estimator for an E_b/N_0 of 10 dB. With the estimation using 20 successive OFDM symbols, the variance is around 10^{-13}, which is sufficient to estimate an error around 10^{-6}. To check the estimator performance, an OFDM simulation chain is implemented using the FFT window correction.

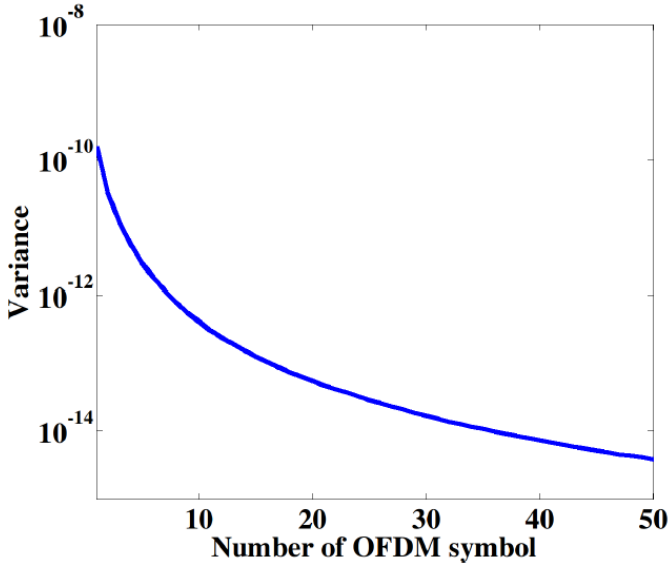

FIGURE 12: VARIANCE OF THE ESTIMATOR ACCORDING TO THE NUMBER OF SYMBOL M.

Fig. 13 shows the BER according to the OFDM symbol number for different error values. To guarantee a sufficient variance, the FFT correction is done every 20 OFDM symbols. It is possible to correct the FFT less frequently, but it makes the BER less stable according to the OFDM symbol number. However, the BER is stable in the case where the error is equal to 1 ppm. The more the error value increases, the more the correction is irregular until the divergence of the system with the error of 30 ppm. When the error is 5 ppm, the increase of the BER is low which allows us to consider an operating margin for the synchronization system.

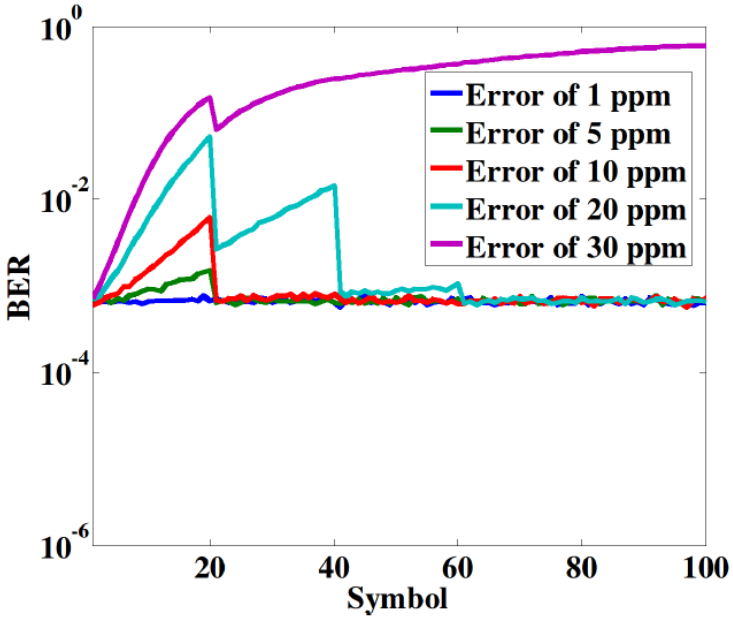

FIGURE 13: BER ACCORDING TO THE NUMBER OF OFDM SYMBOL.

To check the stability of the system, the simulations during one super-frame have been done and with the different errors of 1, 5 and 20 ppm. These simulations show that the system does not diverge. In this section, it has been assumed that the variation of the local oscillators' drift is around 1 ppm during a super-frame. If the error increases, it will imply rough correction for the receiver after 20 OFDM symbols. To avoid that, it is possible to use loop filters. These filters allow to smooth the correction system to improve the stability of the PLC system in reception. However, if the variation is too significant, for example 30 ppm, the system will diverge. In this case, it is necessary to use aircraft security strategies as redundant systems to ensure very high security level.

VI. CONCLUSION

In this paper a sampling frequency synchronization system has been proposed for a PLC system in the FCS aeronautic environment. To solve the FFT drift of the OFDM communication system, the sampling frequency synchronization system is performed in two phases. The first one is the initialization phase during the switching of the aircraft, which allows precise channel estimation and synchronization based on conventional OFDM receiver algorithms. The second one, is the correction of the FFT drift using the phase of the received data every 20 OFDM symbols. To do that, two estimators using the maximum likelihood have been proposed. The first one estimates the sampling frequency offset of one OFDM symbol. The second one estimates the sampling frequency offset of 20 OFDM symbols using the estimation of the first estimator. This estimation allows to have a stable and simple synchronization system up until 20 ppm of drift between transmitter and receiver oscillators. To increase the robustness of the synchronization strategy, a super-frame structure is proposed, which allows a re-estimation of the channel and a resynchronization with an accuracy of one ppm at the beginning of each super-frame. The interest to consider a super-frame is to have a long stable period and propose a simple synchronization system during the operating phase.

ACKNOWLEDGEMENTS

This study has been funded by Safran.

REFERENCES

[1] T. Pollet and M. Moenneclaey, "Synchronizability of OFDM signals", in Global Communications Conference, vol. 3, pp. 2054–2058, November 1995.

[2] B. Ai et al., "On the synchronization techniques for wireless OFDMsystems," IEEE Trans. on Broadcasting, vol. 52, no. 2, pp. 236-244, 2006.

[3] G. Gao et al., "Robust Preamble Design for Synchronization, Signaling Transmission, and Channel Estimation," IEEE Trans. on Broadcasting, vol. 61, no. 1, pp. 119–126, 2015.

[4] T. Pollet and M. Peeters, "Synchronization with DMT modulation," IEEE Communications Magazine, vol. 37, no. 4, pp. 80–86, 1999.

[5] J. A. Cortes, L. Diez, E. Martos, F. J. Canete, and J. T. Entrambasaguas, "Analysis of timing recovery for DMT systems over indoor power-line channels," in IEEE Global Communications Conference, Nov. 2006, pp. 1–6.

[6] Y. Chen et al., "A new preamble design and pattern matching aided timing synchronization for PLC," in International Conference on Communications and Networking in China, pp. 44–47, August 2014.

[7] D.K. Kim et al., "A new joint algorithm of symbol timing recovery and sampling clock adjustment for OFDM systems", IEEE Trans. on Consumer Electron., vol. 44, pp. 1142–1149, August 1988.

[8] S.Y. Liu and J.W. Chong, "A study of joint tracking algorithms of carrier frequency offset and sampling clock offset for OFDM based WLANs", in International Conference on Communications, Circuits and Systems and West Sino Expositions, pp. 109–113, June 2002.

[9] H.S. Chen and Y. Lee, "Novel sampling clock offset estimation for DVB-T OFDM ", Vehicular Technology Conference, pp. 2272–2276, October 2003.

[10] M. Schmidl and D.C. Cox, "Robust frequency and timing synchronization for OFDM", IEEE Trans. On Communications, vol. 45, no. 12, pp. 1613–1621, December 1997.

[11] M.Morelli and U.Mengali, "An improved frequency offset estimator for OFDM applications", IEEE Communications Letters, vol. 3, no. 3, pp. 75–77,March 1999.

[12] H. Minn, V.K. Bhargava and K.B. Letaief, "A robust timing and frequency synchronization for OFDM systems", IEEE Trans. OnWireless Communications, vol. 2, no. 4, pp. 822–839 July 2003.

[13] K. Shi and E. Serpedin, "Coarse frame and carrier synchronization of OFDM systems: A new metric and comparison", IEEE Trans. onWireless Communications, vol. 3, no. 4, pp. 1271–1284, July 2004.

[14] M. Crussière, J.-Y. Baudais, J.-F. Hélard, "A novel joint and iterative scheme for synchronization and channel estimation in MC-CDMA power line communications", in Vehicular Technology Conference, vol. 3, pp. 1723–1727, September 2004.

[15] M. Segvic, K. Krajcek, and E. Ivanjko, "Technologies for distributed flight control systems: A review," in International Convention on Information and Communication Technology, Electronics and Microelectronics, Opatija, Croatia,May 2015, pp. 1060–1065.

[16] T. Larhzaoui et al., "Analysis of PLC channels in aircraft environment and optimization of some OFDM parameters", in International Conference on Systems and Networks Communications, pp. 65–69, October, 2013.

[17] T. Larhzaoui et al., "OFDM PLC transmission for aircraft flight control system," in International Symposium on Power Line Communications and its Applications, pp. 220–225,March-April 2014.

[18] S. Kay, Fundamentals of statistical signal processing, Prentice Hall, Signal Processing Series, 1993.